ELSEVIER

International Journal of Mass Spectrometry 206 (2001) 231–244

International Journal of Mass Spectrometry

Time-of-flight mass analyser for anion mass spectrometry and anion photoelectron spectroscopy

U. Boesl,* C. Bäβmann, R. Käsmeier

Institut für Physikalische und Theoretische Chemie, Technische Universität Munchen, Lichtenbergstrasse 4, D-85748 Garching, Germany

Received 23 February 2000; accepted 2 August 2000

Abstract

The ion optical design and characteristic features of a time-of-flight mass analyser for anion mass spectrometry and, in particular, for anion photoelectron and anion zero kinetic energy electron spectroscopy are described. A special design was necessary to avoid the formation of electrons and neutrals by collisions of anions with any kind of surfaces on their way to and through the photoelectron spectrometer and to the ion detector. (Int J Mass Spectrom 206 (2001) 231–244) © 2001 Elsevier Science B.V.

Keywords: Time-of-flight mass spectrometry; Negatively charged ions; Anions; Photoelectron spectroscopy; Photodetachment

1. Introduction

Anion mass spectrometry delivers complementary information to cation mass spectrometry from a viewpoint of analytical studies as well as of basic research [1–5]. Similarly, anion photoelectron spectroscopy (for a review see [6]) delivers complementary molecular information to conventional photoelectron spectroscopy. The latter involves neutral–cation transitions and primarily supplies data about cationic energy levels, the former involves anion–neutral transitions and allows the study of neutral molecular states. However, in contrast to conventional photoelectron spectroscopy, the initial systems of anion photoelectron spectroscopy are charged particles and can be analysed prior to spectroscopy. In other words, anion photoelectron spectroscopy has the unique and intrinsic feature of supplying mass selected spectroscopic information on neutral molecular systems.

This article deals with the mass analyser necessary for such types of experiments. Various types of mass spectrometers on the basis of magnetic fields, electrostatic fields, or both, have been applied for mass separation. Most commonly, linear Wiley-McLaren-type time-of-flight mass analysers are used, where the accelerated ions are separated in time according to their mass-dependent flight times in a field-free drift region. The so-called “space focus” is a particular point in this drift region, where the ion pulses are compressed in the direction of ion trajectories and which, therefore, represents a position of high mass separation. This is the point of choice to record mass spectra or perform photodetachment at high mass resolution. In some experiments also a space-saving quadrupole mass spectrometer or a Wien velocity

* Corresponding author. E-mail: Ulrich.boesl@chitum.de

PII S1387-3806(01)00313-4

filter is incorporated for mass separation. The latter has been used in the very early anion photoelectron experiments [7] and still is used by Lineberger and co-workers [8] and other groups [9]. Magnetic sector, quadrupole or Wien filter are well adapted to continuous anion sources, whereas time of flight mass analysers are optimally combined with pulsed anion sources. Many research groups working in the field of anion photodetachment and anion photoelectron spectroscopy are using these latter means of mass separation [10–14].

Here, we describe a time-of-flight mass separator particularly designed for anion mass spectrometry and anion photoelectron spectroscopy, which enabled us to measure anion photoelectron and highly resolved anion zero kinetic energy electron (ZEKE) spectra of various types of molecular anions [15–19]. The conditions to be fulfilled are (1) an appropriate anion source, (2) sufficient mass selection, (3) suppression of disturbing electrons and neutrals, and (4) the possibility to photodetach electrons from anions in a mass selective way. As for the anion source, it has been extensively described elsewhere [20]. Mass selection is achieved in a linear time-of-flight analyser, as described in more detail below. Near the space focus of the ion source optics of this mass analyser, mass selective photodetachment for photoelectron spectroscopy is possible. A linear instead of a reflectron time-of-flight mass spectrometer has been used to detect neutrals from the photodetachment in correlation with the anion mass spectrum.

2. Influence of background electrons

It turned out, that background electrons (whose sign of charge is the same as that of anions), may disturb anion mass spectra and photoelectron spectra considerably. This is illustrated by the mass spectrum of chlorine anions in Fig. 1. Although at masses 35 and 37 the anion peaks of chlorine appear as expected, additional strong peaks show up at flight times, which do not correspond to well-defined masses. These signals are released from three grids in front of the anion detector by collisions of chlorine anions. Due to

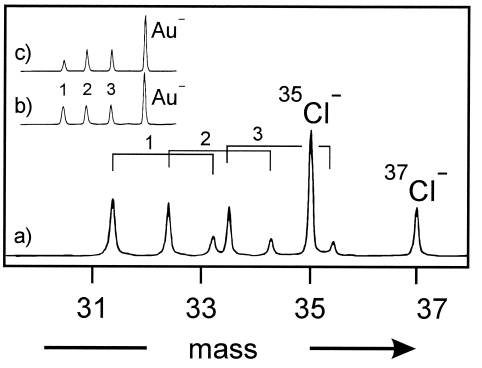

Fig. 1. The appearance of electrons released due to collisions of primary anions with three grids (1, 2, 3) mounted in front of the ion detector: a) Mass spectrums of chlorine anions, b, c) mass spectrum of gold anions. c) grid 1 (in a and b made out of copper) has been replaced by a gold grid. The secondary electron emission is reduced considerably.

their small mass and postacceleration between grids and detector surfaces, the electrons arrive prior to the anions which have caused their production. Because electrons are released by both isotopes of chlorine, this gives rise to a complicate system of signals. The secondary electrons from one particular grid are marked by a horizontal rectangular bracket and a number corresponding to the grid position in front of the detector. If considering the fact, that the optical transmission of the grids was $>90\%$, the electron signals are astonishingly large. This might be due to an electron production yield at the grid of larger than 1 and to a better sensitivity of the channel plate detectors for electrons than for ions.

This large yield can be used for transient detection of masses. Thus, a thin wire (0.1 mm thickness) may reduce the ion intensity only by few percent but supply a mass spectrum prior to further ion experiments [21]. To study the origin of these secondary electrons, the material of grid 1 has been varied. To simplify the spectrum, gold anions have been used (see inset b and c in Fig. 1). Although in Fig. 1(b) all three grids were made out of copper, in Fig. 1(c) grid 1 is out of gold. A considerable reduction of the secondary electron yield is observed for grid 1. Further experiments [22] proved, that not the work function but the ability of the metal surface of

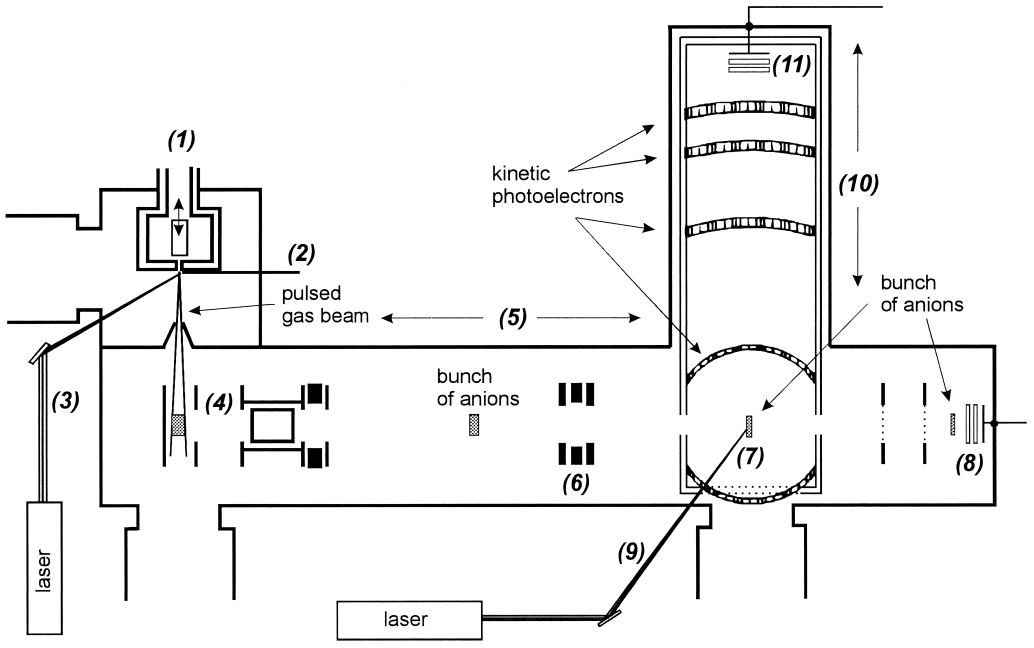

Fig. 2. Experimental set-up of the time-of-flight mass analyser with anion source and photoelectron spectrometer. (1) pulsed supersonic beam value, (2) metal wire for supplying photoelectrons after irradiation by laser (3). (4) ion source optics; (5) field free drift tube for time-of-flight mass separation; (6) mass gate; (7) space focus of the pulsed ion source and point of photodetachment; (8) multi-channel plates detector for recording primary anions and/or secondary neutrals; (9) detachment laser; (10) field free drift tube for measuring electron kinetic energy (time-of-flight photoelectron spectrometer); (11) electrons.

absorbing residual gas molecules is responsible for this effect. Thus by heating a thin stainless steel wire up to about 700 K, the electron production could be suppressed nearly totally. After switching off the heating, the electron signal recovered within 100 s. This indicates, that secondary electrons are produced by collisions of primary particles with surface adsorbed residual gas molecules. It was found, that the state of charge of the primary particles does not influence the electron yield remarkably and similar results are obtained for anions, neutrals, or cations. As a consequence, the experimental apparatus has to be designed such that collision of primary anions with any kind of surfaces is avoided. This concerns the ion source optics as well as the mass gate, used prior to photoelectron spectroscopy, and the photoelectron spectrometer. The effect of grids in front of the ion detector can be suppressed by applying appropriate voltages to these grids.

3. Experimental setup: overview

Fig. 2 displays an overview of the apparatus, including anion source, time-of-flight mass separator and time-of-flight photoelectron spectrometer. (The numbers in parentheses used in this section correspond to the numbers given in Fig. 2.) Anions are produced in a pulsed supersonic molecular beam. This is formed by expanding a special gas mixture (whose composition depends on the molecular systems of interest) through a periodically opened nozzle (1) into the vacuum. Very near to the nozzle, a metal wire (2) is mounted. It serves as the source for photoelectrons with small kinetic energy emitted after irradiation by a laser pulse (3). Electron attachment, followed by dissociation, by molecular cooling due to collisions in the supersonic beam, by further chemical reactions, or by cluster formation finally results in the production of the wanted anions. Depending on the type of

molecular system to be studied (short lived radicals, weakly bound van der Waals clusters, chemical intermediates, or stable molecules) few species of anions or a whole manifold of different anionic species is formed. For more details of the laser induced anion source see [20].

The whole bunch of neutral gas molecules and ionised species drifts down into the ion source optics (4). A pulsed voltage, which is synchronised in time with the gas pulse, is applied to the repelling electrode and the anions are extracted into the time-of-flight drift region (5). After about two thirds of the drift length of the anions from the ion source optics to the point of photodetachment, a special mass filter (6) is mounted. This mass filter is necessary for the case when the anions of interest for photoelectron spectroscopy are preceded by an intense anion bunch of a slightly smaller mass. If not deflected, these anions would give rise to secondary electrons by collisions with nearby surfaces and thus disturb the photoelectron spectra. The ion source optics (4) is designed so that radial as well as transversal focusing of the anion beam at the point of photodetachment (7) is achieved. Elements (4) and (6) are particularly designed to prevent anions from striking any kind of surface and form fast neutrals, which cannot be influenced by electric fields anymore, and background electrons. Anion mass spectra are recorded by a channel plate detector (8). The distance between the point of photodetachment (7) and anion detection (8) is as small as possible to achieve reasonable mass resolution at both positions.

Photodetachment (7) is achieved by a second laser pulse (9). Either the higher harmonics (532, 355, or 266 nm) of a Nd:YAG laser, or tuneable laser light from a dye laser or an OPO (optical parametric oscillator) laser source may be used. For photoelectron spectroscopy tuneable laser light is optional. It allows small excess energies of laser photons above the energy range of interest and therefore small kinetic energies of the released photoelectrons. Slow electrons, on the other hand, can be energy analysed with considerably increased resolution in time-of-flight energy analysers. Such a time-of-flight energy analyser for photoelectrons (10) consists of a field-free drift region which is shielded against magnetic fields by a double walled μ-metal tube. The kinetic electrons arrive at the electron detector (11) (channel plate detector) at flight times, which are reciprocally proportional to the square root of their energy and reflect their binding energy, and the energy levels in the residual neutral molecule, respectively. For high resolution ZEKE spectroscopy tuneable laser light is intrinsically necessary. Up to now, anion ZEKE spectroscopy has been performed by few research groups, only [10,15,23].

4. Ion source optics

The ion source optics (4) (see Fig. 2) has been designed and tested with the help of computer simulations [24]. Together with an illustration of its focusing characteristics, it is displayed in Fig. 3 in more detail. The ion optics consists of two electric fields. The first field is determined by the voltages *U*rep and *U*attr of the anion repelling and attracting electrodes, with *U*rep in the range from -600 V to -1.2 kV and a ratio *U*rep/*U*attr of roughly 2–3. The second field is kept homogeneous by a set of equidistant electrodes whose first is the attracting electrode and whose final one is grounded. The distance of the repelling and attracting electrode is 20 mm, whereas that of the attracting and the final electrode in the second electric field is 82 mm. The electrode diameter is 90 mm, the diameter of the circular open area in the centre of the electrodes is 10 mm. The first electric field is determined by a grid on the side of the attracting electrode. This is the only grid of the ion source optics; there are no more grids in the second field. Fine tuning of the voltages here allows a very gentle radial focusing (see enlarged scheme of ion optics with ion trajectories) which has two purposes. The first is keeping the anions away from the edges of the electrodes. This avoids the formation of unwanted electrons and fast neutrals. The latter cannot be influenced by electric or magnetic fields anymore and may produce electrons in an uncontrollable way (see Sec. 2). The second purpose is keeping the anion beam parallel over a long distance.

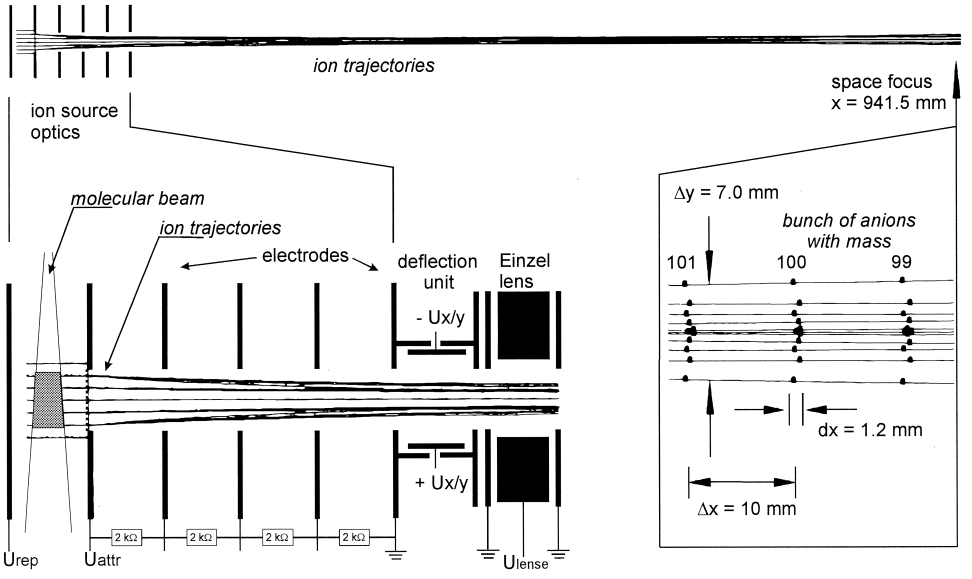

Fig. 3. Ion source optics with computer simulation of the anion trajectories. Inset: the region of the space focus displayed on an about 120 fold enlarged scale showing three separate ion bunches of mass 99, 100, and 101.

If the molecular beam (transporting anions from the anion source into the ion optics) passes the first electric field centrally between the repelling and attracting electrodes, then the flight path lengths of the anions within the ion source optics are 10 and 82 mm, respectively. However, the width of the molecular beam at the position where the anions are extracted is large (in the range of 10 mm). The widely spread anion start positions cause a large distribution of final ion kinetic energies as well as path lengths of acceleration. The question arises if the ion optics described up to now allows one to achieve a satisfying "longitudinal" focusing (space focus) despite this large ion energy spread and a long enough flight path length to this space focus. The long flight pass length is necessary for a good mass separation at the point of photodetachment [see (7) in Fig. 2]). We found a reasonable distance between the exit electrode of the ion source optics and the space focus of about 95 cm. In Fig. 3, ion trajectories are displayed, found by computer simulations [24] for the described ion optics and the supposed space focus. Ions starting at five different *y* positions (vertical to ion extraction direction) and three different *x* positions have been considered. The initial velocity distribution of the anions in the direction of ion extraction is negligible to the vertical orientation of the molecular beam. Even the vertical velocity component is only a thermal one and can be corrected for by deflection plates. Because ion densities are fairly small space charge usually does not play a significant role either. On the right-hand side, a strongly enlarged view of the space focus region is shown. Ion packages of the three masses 101, 100, and 99 are shown. With the black spots at the left and right edge of an ion bunch representing an average spread [i.e. full width at half maximum (FWHM)] then the width dx of one ion bunch and the distance Δx of two neighboured ion bunches may be an indication for the mass resolution $R(50\%)$ achievable at the space focus. One way to calculate $R(50\%)$ is: $R = M\Delta t/dt$ with Δt the difference of flight times of neighboured masses $M$and $M + 1$ and dt the width of a mass peak due to one ion package. Since $\Delta t/dt \approx \Delta x/dx$, one finds from Fig. 3 a estimated mass resolution of 850.

In Fig. 4, a mass spectrum [Fig. 4(a)], measured at the space focus of the ion source optics described previously and a small part (range of four mass units)

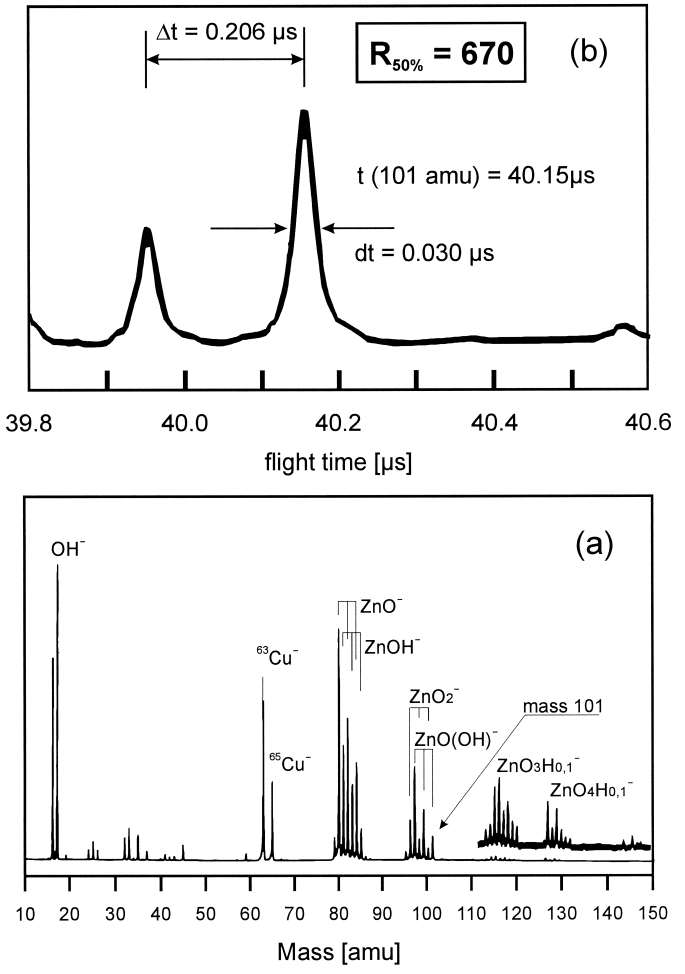

Fig. 4. Mass spectrum measured at the space focus. (a) With the wire (2) (see figure 2) made out of brass, anionic copper and zinc complexes appear in the mass spectrum. (b) The mass range between mass 99 and 103 is shown on an enlarged mass scale for determination of the mass resolution.

of a measured anion flight time spectrum [Fig. 4(b)] are shown. Using flight times and peak widths from Fig. 4(b), an experimental value of the mass resolution will now be deduced. The highest peak in Fig. 4(b) is due to mass 101. This mass peak is marked in the mass spectrum below [Fig. 4(a)] and is a member of a group of mass peaks which are due to the anions of ZnO_2, ZnO(OH), and their zinc isotopes. The whole mass spectrum is measured by using the anion source (see (1) in Fig. 2) with the wire (see (2) in Fig. 2) made out of brass. This wire served as a supplier of electrons at laser induced photoelectron emission, but also released copper and zinc atoms. The equation $R = M\Delta t/dt$ delivers a value of $R(50\%) = 670$ for mass 101 with the experimental values of $\Delta t(100/101) = 0.206$ μs and $dt(\mathrm{FWHM}) = 0.030$ μs. In time-of-flight mass spectrometry, also the equation $R = (1/2)t/dt$ is a valid formula for the mass resolution. With the measured flight time t ($M = 101$) = 40.15 μs and $dt = 0.030$ μs, $R(50\%) = 690$ is obtained, in good agreement with the above value of 670.

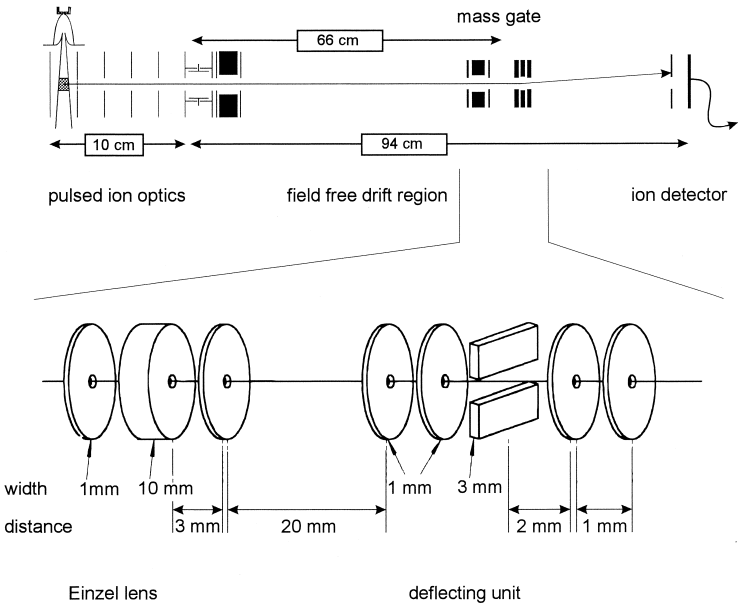

Fig. 5. The mass gate consisting of an Einzel lens and a deflecting unit. It is used to prevent intense ion bunches from inducing back ground electrons and neutrals which could disturb the mass spectra and photoelectron spectra of following smaller ion bunches of higher mass.

5. Mass gate prior to photodetachment

Let us assume the following case: the bunch of anions with the mass of interest is of relatively low intensity and other bunches of anions with very similar mass ($\Delta M \geq 1$) but with considerably higher intensity precede these anions on their way through the time-of-flight spectrometer. Now if photoelectrons detached from the anions of interest are to be studied then stray electrons from the intense preceding ion bunch (e.g. few or even less than 1% of these ions may hit surfaces at the entrance to the photoelectron spectrometer) contribute a strong background signal. This may be strong enough that photoelectron spectroscopy of weak anion peaks cannot be performed anymore although the sensitivity of the photoelectron apparatus would be sufficient.

To overcome this problem, a mass gate is used in front of the point of photodetachment (in the space focus). This mass gate setup is displayed in Fig. 5 and consists of two elements, an Einzel lens to refocus the ion beam and a deflecting unit. The whole assembly is positioned 66 cm after the ion source exit electrode where the ion beam has a waist (see Fig. 3). The deflecting unit is a specially designed set of two bars with two grounded shielding electrodes in front and behind it. Between the two bars a pulsed voltage is applied which is able to deflect ions out of their original ion trajectory far enough so that they are stopped at a stopping electrode.

The need for a special design is due to two conditions. In the whole assembly, a minimum of surface collisions should occur which could give rise to noncontrollable fast neutrals and irregularly distributed electrons (same argument as for the second electric field of the ion source optics; see also Fig. 1 as an example of what should not happen). This condition is fulfilled by the position of the whole assembly at the ion beam waist, the additional Einzel lens, and electrodes with a large central opening of 10 mm diameter. This diameter is a compromise between a wide transit opening for the ions and a small and therefore efficient gap between the deflecting bars (central electrode).

The second condition is related to mass selectivity. In the worst case the disturbing ion bunch is due to ions with a mass $M - 1$. If the mass M of the ions of interest is 101, a selectivity of 100 would be neces-

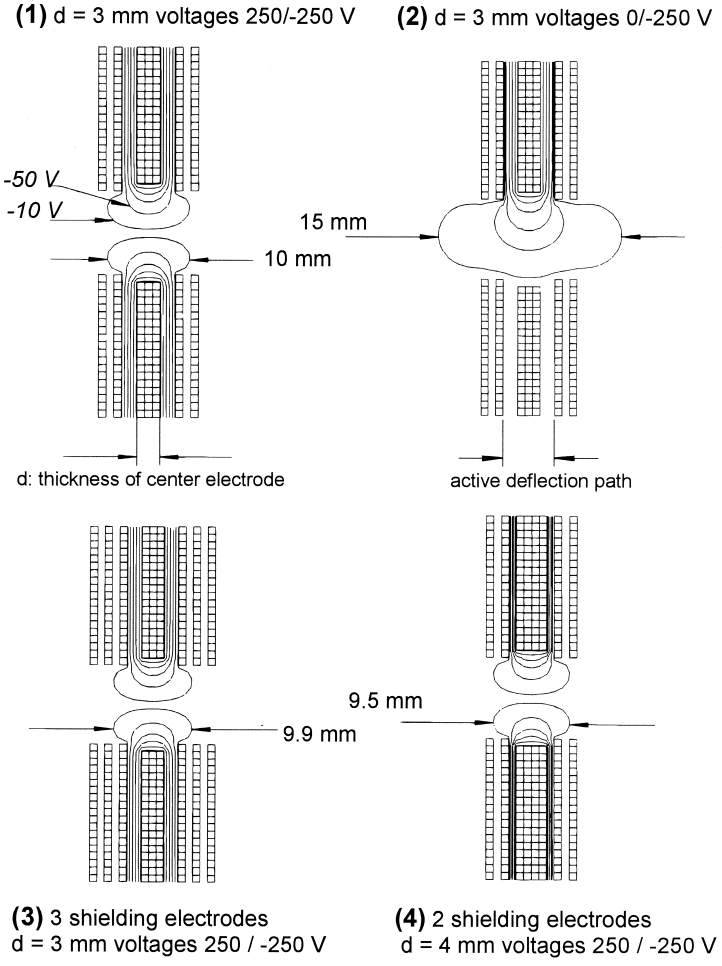

Fig. 6. Four versions of deflecting units for the mass gate differing of shielding electrodes, thickness of centre electrode or way of applying voltages to the centre electrode. Version (1) is the best compromise between deflecting power and minimum disturbance of the field free drift region.

sary. In reality, the selectivity condition is less stringent because a strong reduction of the corresponding ion bunch is mostly sufficient with no need for a total depletion. Nevertheless, to achieve sufficient mass selectivity, the path length where the ions are subjected to a deflecting electric field has to be minimised in size and the surrounding field-free drift region should not be spoiled by residual small leaking fields. The former is achieved by keeping the active deflection path 6 mm long (this turned out to be an optimum from various SIMION simulations). The latter condition is fulfilled by applying the same voltages but with opposite sign to both bars. Possible small fields leaking out of the shielding electrodes then cancel each other [compare case (1) and case (2) in Fig. 6]. An additional set of shielding electrodes [see (3) in Fig. 6] did not cause a further improvement. Also, a wider central electrode [see (4) in Fig. 6] with the same active deflection path length did not improve the situation considerably, but resulted in a worth deflecting power.

Finally, we found the deflecting unit design (1) (Fig. 6) to be the optimum for our purposes. For instance, let us assume that mass 100 should be deflected so that they do not disturb photoelectron studies on mass 101. Since both ion bunches are

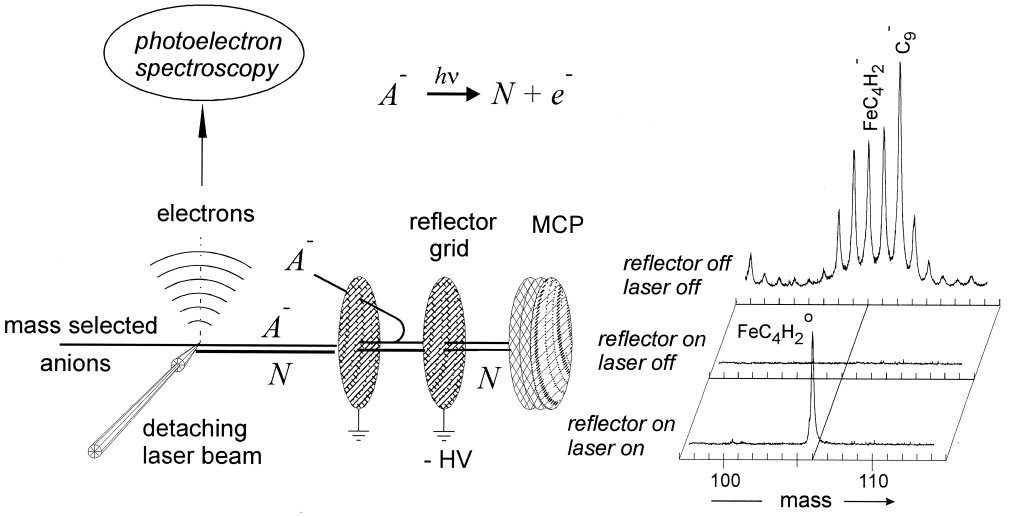

Fig. 7. Illustration of mass selected laser induced photodetachment by a three step experiment (i) anion reflector off, laser off, (ii) anion reflector on, laser off, (iii) anion reflector on, laser on. Clearly, only one mass is hit by the detaching laser. The released photoelectrons are entering the photo electron spectrometer.

separated by about 6 mm (10 mm at the space focus, see Fig. 3), mass 100 will leave the active deflection path just when mass 101 is entering it. Synchronising the pulsed deflection field with the transit of mass 100 will allow to sufficiently suppress the electron background signal induced by these ions and disturbing experiments on ions with mass 101.

6. Mass selective photodetachment for anion photoelectron spectroscopy

In Fig. 7, an experiment has been performed which illustrates how mass selective photodetachment is achieved. A special grid arrangement in front of the ion detector is used, which allows to reflect charged particles and therefore to distinguish between charged and neutral molecules.

On the right-hand side three different mass spectra are displayed resulting from three different experimental situations. In the first case (reflector off, laser off) the anions are recorded after passing the field-free drift region (conventional time-of-flight mass spectrum). The mass spectrum shows a group of iron carbon hydrides (i.e. FeC_4H_i, $i = 0-6$) superimposed on mass 108 and 109 by C_9^- and C_9H^-. Both types of species are formed, when an iron wire is positioned in front of a supersonic beam nozzle with a laser pulse focused on it. In addition, the carrier gas of the supersonic beam consisted of argon (3 bar) seeded with acetylene. For further details, see [20].

If a negative high voltage is now applied to the reflector grid in front of the multichannel plate ion detector, then anions cannot reach the detector, and the mass spectrum simply reveals the base line (see second mass spectrum: reflector on, laser off). In the third experimental step, a detaching laser beam is focused into the space focus. It is synchronised with the transit of the anion $FeC_4H_2^-$ through the space focus. This laser excitation results in the detachment of an electron from this ion of mass 106, solely. The residual neutral molecule, however, will now pass the reflector grid and reach the multichannel plate detector. Therefore, the third mass spectrum (reflector on, laser on) reveals a single mass peak.

This procedure can be used to confirm that the photodetached electrons actually are due to the anion which was requested to be studied. On the other hand, by recording the intensity of the residual neutrals

(here $FeC_4H_2^0$) as a function of the detaching laser wavelength, a photodetachment spectrum can be measured, which delivers values for the electron affinity. This is comparable to photoionisation spectroscopy, which supplies information about the ionisation threshold. Due to the intrinsic shape of the corresponding spectra (i.e. step functions), vibrational information about the neutral, respectively, molecular cation (photoionisation spectra) is mostly inaccessible being hidden under a strong background signal.

This is not the case when studying the kinetic energy of the released electrons in photoionisation, as well as in photodetachment spectroscopy. There exist three widely spread types of instruments to measure the kinetic energy of electrons. The most uncomplicated arrangement is a time-of-flight photoelectron spectrometer. Its advantage is a relatively good energy resolution. For a review of laser induced photoelectron analysers see [25]. A great disadvantage is the small acceptance angle and thus a small collection efficiency for photoelectrons. This problem is avoided in the second type of analyser, the magnetic bottle electron spectrometer [26]. Its high collection efficiency of nearly 100% is achieved by using magnetic fields guiding the emitted electrons. However, collecting electrons from all directions causes large differences in flight paths and thus flight times resulting in a reduced energy resolution. For experiments using continuously operating sources (e.g. flowing afterglow) a hemispherical electrostatic energy analyser is suitable. The electrons travel in the field between a section of two concentric spheres. Only those, that pass the entrance slit are detected, have a certain kinetic energy and therefore move on a distinct spherical trajectory which enables them to pass the exit slit.

A time-of-flight spectrometer is used in our apparatus. The starting time of the electrons is determined by the event of photodetachment (and thus the laser pulse). The flight time in a fully field-free drift region reflects the kinetic electron energy. For shielding the drift region from external electric and magnetic fields, it is surrounded by a double-walled μ-metal tube which is closed by a μ-metal cap at the electron detector side and by a μ-metal grid, on the side of the vacuum pump. A set of three multichannel plates is used as an electron detector. A particular high-resolution spectroscopy involving photoelectrons is ZEKE [27], and anion ZEKE spectroscopy [10,19], respectively. In contrast to conventional photoelectron spectroscopy, here tuneable lasers are needed and the intensity of the so-called ZEKE electrons are measured as a function of laser wavelength. Spectroscopic resolution of 0.1 cm^{-1} (ZEKE spectroscopy) and 1.5 cm^{-1} (anion ZEKE spectroscopy) have been achieved.

7. Mass selective anion photoelectron spectra

In this section some examples of anion photoelectron spectra are displayed where the ion source optics and mass separation described previously have been used. In Fig. 8, the influence of the mass gate on the quality of anion photoelectron spectra is illustrated. The goal was to measure the anion photoelectron spectrum of the water cluster $OH(H_2O)$. The result without a mass gate is shown in the upper part of Fig. 8. The mass spectrum of $OH(H_2O)^-$ is shown as an inset. Due to the ion source conditions a high O_2^- concentration is present and thus the $OH(H_2O)$ anion is preceded by a very intense ion peak whose ion mass is only a few mass units smaller than that of $OH(H_2O)$. The background electrons, produced by this large anion peak, are obvious when comparing the spectra with the mass gate switched off and switched on (lower spectrum in Fig. 8). Since the electron kinetic energy is measured by time-of-flight, background electrons formed in a pulsed way (as by the O_2^- anion bunch) show up at a special (nonrealistic) electron energy. The lower mass spectrum (signal scale increased by factor of 2) demonstrates the action of the mass gate. In particular van der Waals clusters such as $OH(H_2O)$ are delicate systems which usually give rise to unstructured spectra due to unresolved low frequency vibrations and hot bands. The onset of the anion photoelectron spectrum (transition from the anionic to the neutral electronic ground state), which supplies a value for the electron affinity, therefore is hard to be made out. Disturbance

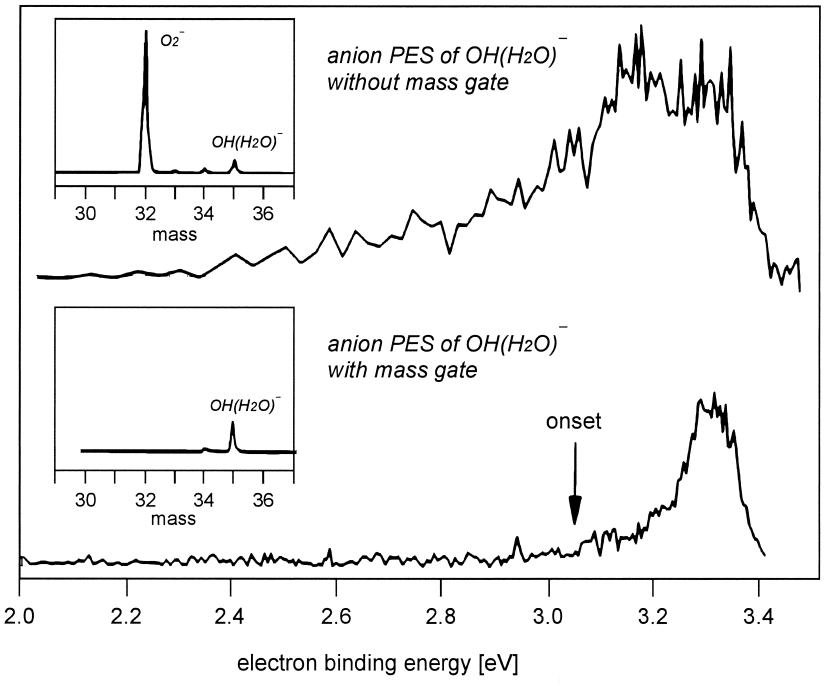

Fig. 8. Photoelectron spectrum of the $OH(H_2O)$ anion. Upper spectrum: mass gate off; Lower spectrum: mass gate on discriminating the O_2-anion. The distrubing effect of the preceding intense anion bunch is evident.

by ambient background electrons would make it impossible to find this origin.

One way to find the electronic origin of an unstructured spectrum of a van der Waals cluster has been used in Fig. 9. The bold line shows the anion photoelectron spectrum of the $O_2(H_2O)$ cluster. In opposition to its water cluster, O_2 (dotted line) exhibits a well-developed structure in its anion photoelectron spectrum. The intensity distribution of the vibrational band is determined by the Franck-Condon factors of the transition. It has been found that for some molecule water clusters [28 –30], the molecular Franck-Condon envelope is preserved in the molecule water clusters whereas the spectral fine structure got lost due to many overlapping bands of van der Waals modes. And in fact, Fig. 9 shows, that the envelope of the O_2^- spectrum fits nicely to that of the water cluster spectrum if shifted by 0.76 eV. It is a reasonable assumption, that also the origin (electron affinity) differs by 0.76 eV. The electron affinity of O_2 has been determined as 0.44 eV [31]. This is also found from the dotted curve in Fig. 9: the vibrational progression begins at 0.45 eV (there is no member of this progression at smaller energies indicating that this is the origin of the spectrum). The bands at lower energies do not fit into the progression pattern. They are due to hot bands and reveal a progression with a significantly smaller vibrational frequency and therefore smaller bond strength of the O_2 anion. A small bond strength is correlated with a large bond length. And indeed, the observed Franck-Condon envelope indicates a strong change of bond length and thus confirms the assignment of the hot bands and the origin of the neutral–anion transition. As a result of these arguments, one finds an electron affinity of 1.2 eV for the $O_2(H_2O)$ cluster and a binding energy of the anionic cluster of 0.76 eV (if neglecting the very small binding energy of the neutral cluster: see the inset in Fig. 9).

Finally, in Fig. 10 an anion ZEKE spectrum is

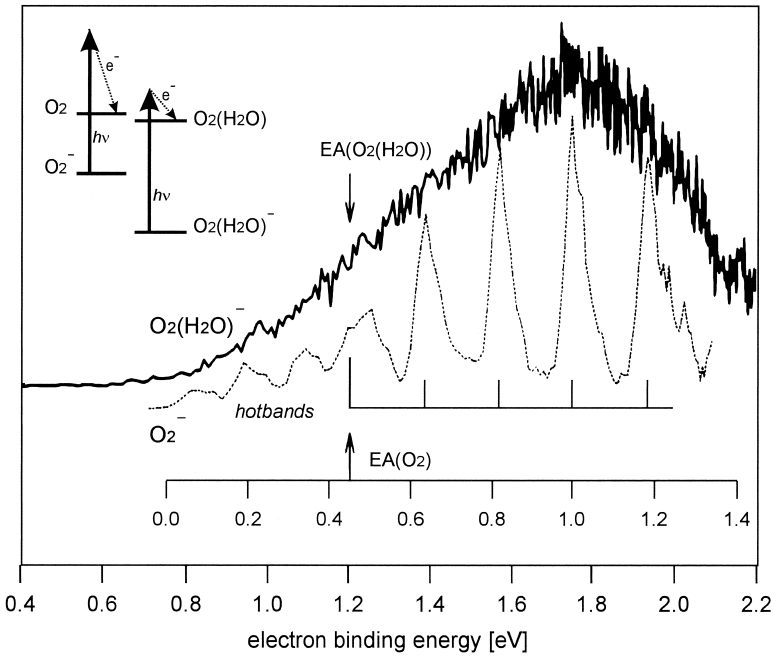

Fig. 9. Anion-photoelectron spectrum of the O_2 anion and the $O_2(H_2O)$ anion. The latter has been shifted by 0.75 eV. The similar envelope justifies the assignment of the electron affinity of the water cluster to 1.2 eV, the same position as the electron affinity O_2 after the shift of the O_2 anion spectrum. The shift, which is just due to the difference of both affinities, is a good estimate for the binding energy of the anionic water cluster (neglecting the small neutral binding energy) as illustrated in the inset.

displayed, where the ion optics and mass separator described previously have been used also. For a detailed description of the ZEKE spectrometer with which the measurements in Fig. 10 have been performed see [19]. ZEKE spectroscopy has originally been introduced as a spectroscopic technique involving cation ← neutral transitions. It mainly delivers information about molecular cations and is distinguished due to its high resolution which is enhanced by several orders of magnitude in comparison to conventional photoelectron spectroscopy. ZEKE spectroscopy involving neutral ← anion transitions is not yet as well known as cation ← neutral ZEKE spectroscopy and it differs in some crucial details from the latter. However, the great benefit of anion ZEKE spectroscopy is that it delivers high resolution data about neutral species which otherwise may not be accessible. This spectroscopy has been applied to molecular systems and van der Waals clusters containing halogen atoms [16,32] to metal and semiconductor clusters [33], to metal carbon hydrides [15], and to chlorine oxides [18] with relevance for atmospheric chemistry. In Fig. 10, an anion photoelectron spectrum (for comparison) and a anion ZEKE spectrum of FeC_2^- are displayed. The latter is well resolved and accurate enough so that exact vibrational frequencies and anharmonicity of the Fe–C stretching vibration in the neutral FeC_2 complex could be measured. This allows the estimation of the dissociation energy of the Fe↔C–C bond to 445 kJ/mol. In addition, the anion ZEKE spectrum reveals small additional peaks that are not resolved in the photoelectron spectrum. They form a short progression with an energy interval of 290 cm^{-1}. Their origin could not yet be assigned. One possibility is that they belong to a different electronic state. It is well known that systems that contain atoms with *d* electrons exhibit energetically low lying and strongly mixed electronic states [17,34].

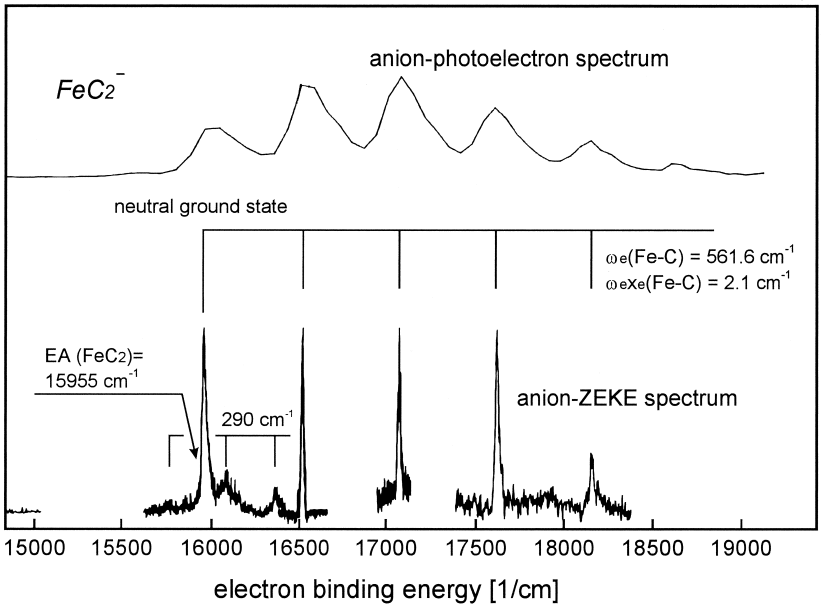

Fig. 10. Anion-photoelectron spectrum and anion-ZEKE spectrum of the anionic FeC_2 complex. The high resolution anion ZEKE spectrum supplies an accurate Fe-C- stretching frequency and its anharmonicity. The latter allows an estimation of the Fe-C-binding energy of about 445 kJ/mol. The additional progression with an interval of 290 cm^{-1} probably is due to an new electronic state which could not yet assigned.

8. Summary

An uncomplicated, but thoroughly designed ion optical device is described which enables anion mass spectrometry and mass selective anion photoelectron spectroscopy to be performed. Attention has been paid to prevent the formation of electrons or fast neutrals due to collisions of anions with any kind of surfaces. The electrons have a charge with the same sign as that of the anions and therefore are accelerated in the same direction and the neutrals cannot be controlled anymore by electric or magnetic fields. Both of them may reach the ion detector or the photoelectron spectrometer and induce background signal or misleading peaks. The ion source optics has been described and the achievable mass resolution has been demonstrated. A special mass gate is presented and the possibility and quality of mass selective photodetachment has been shown. Finally, some examples of anion photoelectron spectra prove the functionality of the linear time-of-flight mass analyser, which is the subject of this article. Hopefully, this description may help other research groups to join the still small community of anion photoelectron spectroscopists.

References

[1] M. Born, S. Ingemann, N.M.M. Nibbering, Mass Spectrom. Rev. 16 (1997) 181.
[2] E. Illenberger, J. Momigny, Gaseous Molecular Ions: An Introduction to Elementary Processes Induced by Ionization, Steinkopff, Darmstadt, 1992, Vol. 2.
[3] J.A. Laramée, P. Mazurkiewicz, V. Berkout, M.L. Deinzer, Mass Spectrom. Rev. 15 (1996) 15.
[4] W.B. Knighton, L.J. Sears, E.P. Grimsrud, Mass Spectrom. Rev. 14 (1995) 327.
[5] V.S. Ong, R.A. Hites, Mass Spectrom. Rev. 13 (1994) 259.
[6] U. Boesl, W. Knott, Mass Spectrom. Rev. 17 (1998) 275.
[7] A. Kasdan, E. Herbst, W.C. Lineberger, J. Chem. Phys. 62 (1975) 541.
[8] P.G. Wenthold, K.-L. Jonas, W.C. Lineberger, J. Chem. Phys. 106 (1997) 9961.
[9] S.T. Arnold, J.G. Eaton, D. Patel-Misra, H.W. Sarkas, K.H. Bowen, in Ion and Cluster Ion Spectroscopy and Structure, J.P. Maier (Ed.), Elsevier Science, Amsterdam, 1989, p 417.

[10] T.N. Kitsopoulos, I.M. Waller, J.G. Loeser, D.M. Neumark, Chem. Phys. Lett. 159 (1989) 300.
[11] C.G. Bailey, M.A. Johnson, Chem. Phys. Lett. 265 (1997) 185.
[12] M. Johnson, K. Kuwatat, C.-K. Wong, M. Okumura, Chem. Phys. Lett. 260 (1996) 551.
[13] J. Fan, L. Lou, L.-S. Wang, J. Chem. Phys. 102 (1995) 2701.
[14] G. Ganteför, M. Gausa, K.H. Meiwes-Broer, H.O. Lutz, Faraday Discuss. Chem. Soc. 86 (1988) 197.
[15] G. Drechsler, C. Bäβmann, U. Boesl, E.W. Schlag, Z. Naturforsch., A: Phys. Sci. 49 (1994) 1256.
[16] C. Bäβmann, U. Boesl, D. Yang, G. Drechsler, E.W. Schlag, Int. J. Mass Spectrom. Ion Processes 159 (1996) 153.
[17] G. Drechsler, U. Boesl, C. Bäβmann, E.W. Schlag, J. Chem. Phys. 107 (1997) 2284.
[18] V. Distelrath, U. Boesl, Faraday Discuss. Chem. Soc., 115 (2000) 161.
[19] U. Boesl, C. Bäβmann, E. Schlag, in Advanced Series in Physical Chemistry: Photoinization and Photodetachment, C.-Y. Ng (Ed.) World Scientific, Singapore, 2000, p. 809.
[20] U. Boesl, C. Bäβmann, G. Drechsler, V. Distelrath, Eur. Mass Spectrom. 5 (1999) 455.
[21] G. Drechsler, C. Bäβmann, W.-D. von Fraunberg, U. Boesl, E.W. Schlag, Rev. Sci. Instrum. 65 (1994) 3172.
[22] W.-D. von Fraunberg, G. Drechsler, C. Bäβmann, U. Boesl, E.W. Schlag, Int. J. Mass Spectrom. Ion Processes 133 (1994) 211.
[23] G. Ganteför, D.M. Cox, A. Kaldor, J. Chem. Phys. 96 (1992) 4102.
[24] D. Dahl, Proceedings of the 43rd ASMS Conference on Mass Spectrometry and Allied Topics, Atlanta, GA, 21–26 May 1995.
[25] K. Kimura, Int. Rev. Phys. Chem. 6 (1987) 195.
[26] P. Kruit, F.H. Read, J. Phys. E 16 (1983) 313.
[27] K. Müller-Dethlefs, M. Sandner, E.W. Schlag, Z. Naturforsch., A: Phys. Sci. 39 (1984) 1089.
[28] G. Markovich, R. Giniger, M. Levin, O. Chesnovsky, J. Chem. Phys. 95 (1991) 9416.
[29] M. Buntine, D. Lavrich, C. Dessent, M. Scarton, M. Johnson, Chem. Phys. Lett. 216 (1993) 471.
[30] J. Eaton, S. Arnold, K. Bowen, Int. J. Mass Spectrom. Ion Processes 102 (1990) 303.
[31] M. Travers, D. Cowles, G. Ellison, Chem. Phys. Lett. 164 (1989) 449.
[32] I.M. Waller, T.N. Kitsopoulos, D.M. Neumark, J. Phys. Chem. 94 (1990) 2240.
[33] C.C. Arnold, D.M. Neumark, J. Chem. Phys. 99 (1993) 3353.
[34] A J. Merer, Annu. Rev. Phys. Chem. 40 (1989) 407.